Multireference Configuration Interaction Study of Dichlorocarbene

ARTICLE *in* CHEMICAL PHYSICS · AUGUST 2015

Impact Factor: 1.65 · DOI: 10.1016/j.chemphys.2015.07.035

6 AUTHORS, INCLUDING:

Bing Yan

Jilin University

47 PUBLICATIONS **63** CITATIONS

Chemical Physics 459 (2015) 54–58

Contents lists available at ScienceDirect

Chemical Physics

journal homepage: www.elsevier.com/locate/chemphys

Multireference configuration interaction study of dichlorocarbene

Erping Sun [a,*], Tingqi Ren [a], Shimin Shan [b], Qixin Liu [a], Haifeng Xu [b], Bing Yan [b]

[a] College of Electronic, Communication and Physics, Shandong University of Science and Technology, Qingdao 266590, China
[b] Institute of Atomic and Molecular Physics, Jilin University, Changchun 130012, China

ARTICLE INFO

Article history:
Received 10 April 2015
In final form 30 July 2015
Available online 5 August 2015

Keywords:
icMRCI+Q
Dichlorocarbene
Equilibrium geometry
Potential-energy surface

ABSTRACT

Dichlorocarbene is an important reactive chemical intermediate, which has received much investigation. However, the energy, structure, and dynamics of the excited states are not well understood. Here, we investigated the equilibrium geometries and energies of seven electronic states, $\tilde{X}^1A_1$, $\tilde{A}^1B_1$, $\tilde{a}^3B_1$, $\tilde{B}^1A_2$, $\tilde{b}^3A_2$, $\tilde{C}^1B_2$ and $\tilde{c}^3B_2$ of CCl_2 using internally contracted multireference configuration interaction method including Davidson correction (icMRCI+Q) with different basis sets aug-cc-pV(X+d)Z(X = T, Q, 5), and the effects of different basis sets on the geometries and energies. For the first time, the theoretical studies of high excited singlet and triplet states of CCl_2 that are related to the lowest three dissociation limits were carried out at the icMRCI+Q/aug-cc-pV(5+d)Z level. The results were compared with the previous experimental and theoretical data where available. Our results will add some understanding and shed some light on the structures and dynamics of electronic states of CCl_2 radical.

1. Introduction

Triatomic halogenated carbenes are important reactive chemical intermediates, playing an important role in the interstellar medium, atmospheric chemistry, gas-phase combustion reactions, and so on [1], which have attracted intense interest of theoretical and experimental studies. The particularly attractive chemistry is their lowest singlet and triplet states which are close in energy but have very different chemistries as a result of their two nonbonding electrons occupying one or two near-degenerate orbitals. Besides, a lot of attentions have been paid to their complicated spectroscopy and photodissociation dynamics in virtue of interactions between the electronic states, like Renner–Teller effect, spin–orbit coupling, and so on. Just as Kable et al. said in their review, halogenated carbenes are model systems for understanding the spectroscopy and dynamics, and valuable benchmarks for comparing experiments with theories [2].

In the past several decades, with the development of high-resolution laser-based spectroscopic techniques and quantum chemistry methods, a large number of carbenes have been investigated, including monohalogenated carbenes CHF [3–8]/CHCl [5,9–11]/CHBr [12,13]/CHI [13], dihalogenated carbenes CF_2 [14–21], CCl_2 [15,22–32], CBr_2 [15,25,33,34], CFCl [35–37], CFBr [34,37–40], CFI [41,42], and so on, using, for example, laser-induced fluorescence spectrum (LIF) [3,14,26,35,40], as well as ab initio calculations [7,13,25,34,38,42,43]. The equilibrium geometries, singlet–triplet energy gaps as well as interactions between the ground state and the lowest triplet state or the first excited singlet state of the carbenes have been studied comprehensively, while much less attention was put on the investigation about the higher excited states which play an important role on the understanding of the laser-induced fluorescence (LIF) spectrum, emission spectrum as well as photodissociation dynamics process in the UV range. To our best knowledge, there are only few reports on the states beyond $\tilde{A}$ state, for example, photodissociation dynamics of CHF and CDF at the $\tilde{B}$ state [4], CCl_2 at 193 nm and 248 nm [28,30–32], and CHCl [44], CFCl [37] and CFBr [37] at 193 nm.

Like all the halocarbenes, the dichlorocarbene, CCl_2, discussed in this paper, has also received much attention. In the past years, the structures of the ground state ($\tilde{X}^1A_1$), the lowest state ($\tilde{a}^3B_1$) and the first singlet state ($\tilde{A}^1B_1$) of CCl_2 as well as singlet and triplet gap (S–T gap) have been extensively investigated by various high-resolution spectroscopic methods [15,24,26,27,29] and quantum chemistry methods [25,45]. The group of Cheong has calculated the molecular structure, vibrational frequencies, and enthalpies of formation of the carbenes CF_2, CFCl, CCl_2 by ab initio quantum chemical methods [26]. Bacskay el al. have calculated the spectroscopic constants of the ground state ($\tilde{X}^1A_1$), the first singlet state ($\tilde{A}^1B_1$) and the lowest triplet state ($\tilde{a}^3B_1$) of the CF_2, CCl_2, CBr_2 carbenes by complete active space self-consistent field (CASSCF), complete active space second-order perturbation (CASPT2), and

* Corresponding author. Tel.: +86 532 86057556.
E-mail address: sunep1005@126.com (E. Sun).

http://dx.doi.org/10.1016/j.chemphys.2015.07.035
0301-0104/

coupled-cluster with single, double and perturbative triple excitations (CCSD(T)) methods with cc-pVTZ basis set [25]. The S-T gap was determined from the photoelectron spectra of $[CCl_2]^-$ in 2002 by McKee and Michl [27]. The electronic transition and interaction between ($\tilde{X}^1A_1$) and ($\tilde{A}^1B_1$) states have been investigated via laser excitation, dispersion fluorescence spectrum by the group of Reid [29].

The studies on the higher excited state of CCl_2 are relatively sparse. In the last ten years, the spectroscopic parameters of seven electronic states including $\tilde{X}^1A_1$, $\tilde{A}^1B_1$, $\tilde{a}^3B_1$, $^1A_2$, $^3A_2$, $^1B_2$ and $^3B_2$ of CCl_2 carbene were studied by the group of Cai using multireference single and double excitation configuration interaction (MRSDCI) methods [22]. Photodissociation dynamics processes at 248 nm [28,31,32] and 193 nm [30] were investigated mainly by Shin and Dagdigian. In these papers, they gave a reliable assignment of the excited electronic state in the 248 nm photodissociation process but were not sure about the state which was excited by 193 nm photon leading to the CCl + Cl fragments.

In this paper, we report calculations on the CCl_2 carbene by high level ab initio methods. The geometry parameters and transition energies of the seven electronic states ($\tilde{X}^1A_1$, $\tilde{A}^1B_1$, $\tilde{a}^3B_1$, $\tilde{B}^1A_2$, $\tilde{b}^3A_2$, $\tilde{C}^1B_2$ and $\tilde{c}^3B_2$) were investigated by internally contracted multireference configuration interaction including Davidson correction (icMRCI+Q) method. The effects of different basis sets on the parameters were also investigated. The potential-energy surfaces of singlet and triplet excited states correlated to the lowest three dissociation limits were studied at the icMRCI/aug-cc-pV(5+d)Z level. The calculations presented here will provide more comprehensive results about the structure and behavior of electronic states of CCl_2 radical.

2. Methods

Ab initio calculations were performed on electronic states of the halogenated carbenes CCl_2, using the Molpro program [46]. In the paper, the geometries of seven electronic states $\tilde{X}^1A_1$, $\tilde{A}^1B_1$, $\tilde{a}^3B_1$, $\tilde{B}^1A_2$, $\tilde{b}^3A_2$, $\tilde{C}^1B_2$ and $\tilde{c}^3B_2$ were investigated by internally contracted multireference configuration interaction (icMRCI) [47,48] method with Davidson correction (+Q) [49]. The active space consists of 18 valence electrons and 12 valence orbitals (18e, 12o) corresponding to $n = 2$ atomic orbitals of the C atom and $n = 3$ orbitals of the Cl atom. The standard uncontracted all electron correlation-consistent basis sets of triple, quadruple and quintuple zeta quality with polarization functions, aug-cc-pVXZ(X = T, Q, 5) [50] and extrapolation to complete basis sets (CBS) limit were employed for carbon and a similar basis set including tight-d functions, aug-cc-pV(X+d)Z(X = T, Q, 5) [51] and extrapolation to CBS for chlorine.

The one-dimensional potential energy surfaces (PESs) of singlet and triplet electronic states about the lowest three dissociation limits of CCl_2 computed at icMRCI+Q/aug-cc-pV(5+d)Z level were given with respect to the angle of Cl−C−Cl, C−Cl distance, respectively, with the other two parameters fixed at their respective equilibrium values. The calculations were carried out in the C_{2v} point group, when the potential energy cuts changed along the Cl–C–Cl bond angle and in the $^{***}C_S$ point group when the potential energy cuts changed along the C–Cl bond length.

3. Result and discussion

3.1. Equilibrium geometries and energies of the seven electronic states

The equilibrium geometries and transition energies (without vibrational zero-point energy) of seven electronic states including the ground state ($\tilde{X}^1A_1$), the first excited singlet state ($\tilde{A}^1B_1$), the lowest triplet state ($\tilde{a}^3B_1$), $\tilde{B}^1A_2$, $\tilde{b}^3A_2$, $\tilde{C}^1B_2$ and $\tilde{c}^3B_2$ state of CCl_2 were calculated using a high-level icMRCI+Q method with different basis sets aug-cc-pV(T+d)Z, aug-cc-pV(Q+d)Z, aug-cc-pV(5+d)Z, and extrapolation to the CBS limit. The results are presented in Table 1. For comparison, available calculations and experimental data reported in the literature are also listed in the table.

The basis sets effects on the geometries and the transition energies are obvious as we see from Table 1. The C–Cl bond lengths decrease as the basis sets increase, while the changes from AV(T+d)Z to AV(Q+d)Z, from AV(Q+d)Z to AV(5+d)Z, or from AV(5+d)Z to CBS are much less pronounced. For example, the C–Cl bond length of the $^3B_1$ state exhibits a decrease of 0.006 Å from AV(T+d)Z to AV(Q+d)Z, a decrease of 0.002 Å from AV(Q+d)Z to AV(5+d)Z, and a decrease of only 0.001 Å from AV(5+d)Z to CBS. The results appear to be well converged with the basis sets increased. By contrast, the Cl–C–Cl angles change differently for different states as the basis sets is increased. The states which have the same configuration have the same trend, for example, the angles for the $^1B_1$ and $^3B_1$ states increase, but decrease for the $^1A_1$ and $^3A_1$ states as the basis sets increase. The transition energies increase as the basis sets increase except for the energy for the $^1B_1$ state. Like the C–Cl bond length, the angles and energies are well converged with the increased basis sets.

To our best knowledge, there is so far experimental data only for the ground state and the first excited singlet state geometries. Our ab initio calculations reproduce the experimental structures quite well. The C–Cl bond lengths are quite well reproduced within 0.001 Å at the icMRCI+Q/aug-cc-pV(5+d)Z level of both the ground state and the first excited singlet state. The bond angles are also in good agreement with experimental data. Calculations on the electronic states of CCl_2 have been carried out by different methods, but there is only one research on the states above the first exited singlet state by Cai et al. at the MRSDCI level [22]. Some differences are found in comparing our calculations with those previous calculations and the largest discrepancy is 0.03 Å for the bond length and 2.2° for the bond angle. In a word, our ab initio calculations are in agreement with the available experimental and theoretical data.

By comparing the geometries obtained from the icMRCI+Q method of the seven electronic states of the CCl_2 carbene, some trends are observed. For the $\tilde{A}^1B_1$ and $\tilde{a}^3B_1$ states, the Cl–C–Cl bond angles are lager, whereas the C−Cl bond lengths are smaller compared with those properties of the ground state. The bond angles of both two states are larger relative to that of the ground singlet state on account of the transition of one electron from the in-plane sp^2-like orbital to an out of-plane p-type orbital on carbon. Due to different electronic transitions, which result in a change of valence shell electron repulsion and s-character of the singly occupied non-bonding orbitals, the geometries of the other four states also are different compared with the ground state. Both the configurations of the $^1A_2$ and $^3A_2$ states are $(1–9a_1)^2(1–2b_1)^2(3b_1)^1(1–6b_2)^2(7b_2)^1(1–2a_2)^2$ corresponding to exciting an electron from $7b_2$ to $3b_1$ in the C_{2v} point group. The C–Cl bond lengths of these two states are about 0.2 Å longer and the Cl–C–Cl bond angles are smaller by about 28°. The configurations of the $^1B_2$ and $^3B_2$ states are $(1–9a_1)^2(1–2b_1)^2\ (1–7b_2)^2(8b_2)^1(1a_2)^2(2a_2)^1$, corresponding to exciting an electron from $2a_2$ to $8b_2$. The C–Cl bond lengths of these two states are about 0.2 Å longer and the Cl–C–Cl bond angles are smaller by about 12°compared with these properties of the ground state.

3.2. High electronic excited states of CCl_2 radical

In the present study, the rigid one dimensional potential energy surfaces (PESs) of singlet and triplet excited states with vertical

Table 1
Equilibrium geometries and Energies of seven states of CCl_2 calculated at the icMRCI+Q level.

CCl_2	aug-cc-pV(T+d)Z	aug-cc-pV(Q+d)Z	aug-cc-pV(5+d)Z	cbs	Previous	
					Calculation	Experiment
$\tilde{X}^1A_1$ *state*						
R_{C-Cl} (Å)	1.725	1.719	1.716	1.716	1.716[a]/1.727[b]/1.722[c]	1.7157[d]
∠Cl–C–Cl (°)	109.33	109.37	109.36	109.33	109.5[a]/109.2[b]/109.9[c]	109.2[d]
$\tilde{a}^3B_1$ *state*						
R_{C-Cl} (Å)	1.680	1.674	1.672	1.671	1.695[a]/1.676[b]/1.672[c]	
∠Cl–C–Cl (°)	127.90	127.90	127.91	127.91	125.7[a]/128.3[b]/128.9[c]	
T_e (eV)	0.892	0.896	0.897	0.899	0.448[a]/0.817[b]/0.742[c]	
$\tilde{A}^1B_1$ *state*						
R_{C-Cl} (Å)	1.661	1.655	1.652	1.652	1.672[a]/1.6858[b]	1.653[e]
∠Cl–C–Cl (°)	131.54	131.64	131.72	131.74	131.5[a]/131.8[b]	131.4[e]
T_e (eV)	2.201	2.186	2.179	2.178	2.326[a]/2.227[b]	2.14 [e]
$\tilde{b}^3A_2$ *state*						
R_{C-Cl} (Å)	1.909	1.899	1.895	1.894	1.947[a]	
∠Cl–C–Cl (°)	81.46	81.45	81.38	81.31	82.6[a]	
T_e (eV)	3.288	3.344	3.360	3.373	3.254[a]	
$\tilde{B}^1A_2$ *state*						
R_{C-Cl} (Å)	1.920	1.910	1.905	1.904	1.962[a]	
∠Cl–C–Cl (°)	81.25	81.23	81.17	81.09	81.4[a]	
T_e (eV)	3.332	3.392	3.408	3.422	3.299[a]	
$\tilde{c}^3B_2$ *state*						
R_{C-Cl} (Å)	1.927	1.915	1.911	1.910	1.950[a]	
∠Cl–C–Cl (°)	97.12	97.08	97.05	97.00	96.0[a]	
T_e (eV)	4.207	4.291	4.317	4.339	4.283[a]	
$\tilde{C}^1B_2$ *state*						
R_{C-Cl} (Å)	1.990	1.978	1.974	1.972	2.020[a]	
∠Cl–C–Cl (°)	95.84	95.77	95.74	95.69	94.7[a]	
T_e (eV)	4.570	4.663	4.692	4.715	4.695[a]	

[a] Ref. [22].
[b] Ref. [25].
[c] Ref. [26].
[d] Ref. [23].
[e] Ref. [21].

transition energy (VTE) up to 8.2 eV of CCl_2, which correlated to the lowest three dissociation limits, were calculated at the icMRCI+Q/aug-cc-pV(5+d)Z level. There is only one theoretical study concerning the electronic states above the $\tilde{A}$ state, in which the electronic spectroscopic constants of seven low-lying electronic states $\tilde{X}^1A_1$, $\tilde{A}^1B_1$, $\tilde{a}^3B_1$, $^1A_2$, $^3A_2$, $^1B_2$ and $^3B_2$ of CCl_2 were calculated at the MRSDCI level by Cai and his coworkers in 1993 [22]. For the states higher than $\tilde{A}$ state, experiments were explored at 308 nm [24], 248 nm [31,32] and 193 nm [30] by different groups using laser induced fluorescence spectrum.

The rigid one dimensional PESs along the C–Cl bond length and Cl–C–Cl bond angle are showed in Figs. 1 and 2 respectively. In each figure, the other two geometric parameters were fixed at their respective equilibrium values. Table 2 lists the results of the VTE, the electron configuration, the oscillator strength, and the transition of each electronic state of CCl_2.

The calculations on the electronic states of CCl_2 along the Cl–C–Cl bond angle were carried out in the C_{2v} point group, and the four different representations are A_1, B_1, B_2 and A_2. As shown in Fig. 1, most of the electronic states of CCl_2 have bent equilibrium geometries, except several excited states which are considered to be linear (or quasi-linear) states with the global energy minima at ~180°, i.e., 1^3A_1, 2^1A_1, 3^1A_1, 2^1B_1 and 2^3B_1. Due to different electronic transitions, the equilibrium bond angles change significantly for different bent states, for example, the ground state 1^1A_1 has an energy minimum at about 110°, while the electronic states 1^1B_1 and 1^3B_1 with the global energy minimum at ~130°, 1^3A_2 and 1^1A_2 at about 80°. Like other triatomic halogenated carbenes,

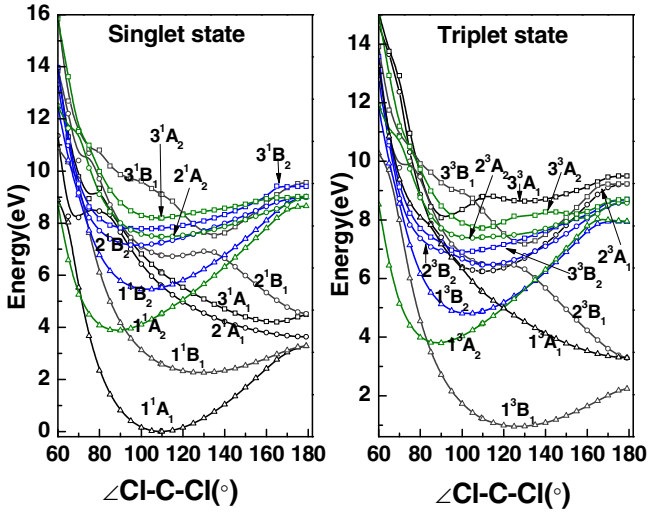

Fig. 1. Potential energy curves of CCl_2 with respect to the Cl–C–Cl bond angle calculated at the icMRCI+Q/aug-ccpV(5+d)Z level. The C–Cl bond lengths were fixed at their respective equilibrium values.

$\tilde{X}^1A_1$ and $\tilde{A}^1B_1$ states are degenerate at linear configuration leading to the Renner–Teller coupling between the states [29].

The calculations on the electronic states of CCl_2 along the C–Cl bond length were carried out in the C_s point group, having two different representations A′ and A″. Like other carbenes, the ground

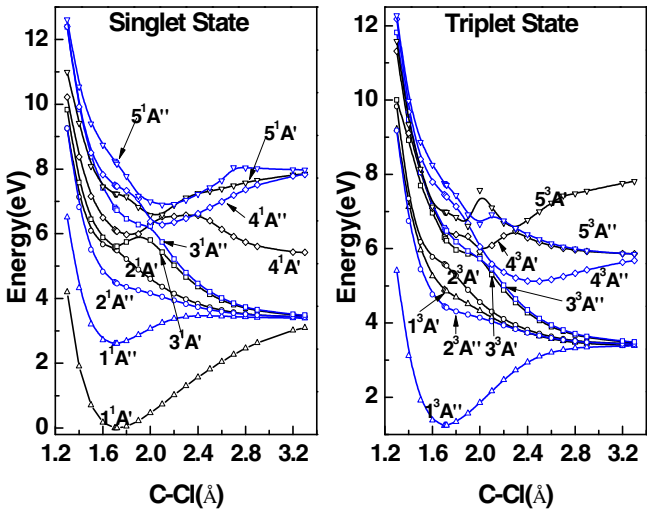

Fig. 2. Potential energy curves of CCl_2 with respect to the C–Cl bond length calculated at the icMRCI+Q/aug-ccpV(5+d)Z level. The other C–Cl bond length and the Cl–C–Cl bond angle were fixed at their respective equilibrium values.

electronic states ($\tilde{X}^1A'$), the first singlet state ($\tilde{A}^1A''$) and the lowest triplet state ($\tilde{a}^3A''$) of CCl_2 are bound states. Most of the remaining states above the first excited singlet state except $4^1A''$, $4^3A''$, $5^1A'$, $5^1A''$ and $5^3A'$ are repulsive, some of which have local minima with different dissociation barriers on their respective potential energy surfaces which may be attributed to the coupling between states with the same symmetry. For example, the coupling in avoided crossing point between $3^1A'$ and $4^1A'$ states leads to the dissociation barrier in $3^1A'$ state. These repulsive potential energy cuts lead to Cl + CCl fragments.

The VTE, the electron configuration, the oscillator strength, and the transition of each electronic state of CCl_2 were studied at the icMRCI+Q/aug-cc-pV(5+d)Z level and carried out in the C_s point group (each state was also labeled with the C_{2v} label and was given in brackets). The calculated VTEs of different electronic states at the $\tilde{X}^1A_1$ state equilibrium conformation are a little higher than the adiabatic excitation energies calculated at the corresponding optimized geometry listed in Table 1. Above the $\tilde{A}^1B_1$ state, the $\tilde{C}^1B_2$ and $\tilde{D}^1A_1$ states are the next two excited states which can be accessed from the ground state by an electric-dipole allowed transition with apparent oscillator strength. They have almost the same VTE (5.516 eV and 5.606 eV) and are close in energy to that of 248 nm photon. Both of the two states may be assigned as the states in the 248 nm photodissociation in Dagdigian's report in 2008 [32]. Their different oscillator strength (0.0748 and 0.00491) may lead the dramatically difference of the 248 nm photon absorption cross section for the zero-point level and excited vibrational levels. The $\tilde{C}^1B_2$ state is purely repulsive and the $\tilde{D}^1A_1$ state possesses a small barrier to dissociation which is attributed to avoided crossing with the higher state (showed in Fig. 2). These properties are consistent with the structureless of the excitation spectra of the CCl fragment in the report. As we can see from Fig. 1, the $\tilde{C}^1B_2$ state has an energy minimum at a slightly smaller bond angle than the ground state while the $\tilde{D}^1A_1$ state prefers a liner geometry as C–Cl bond length increases which may exert a bigger torque on the dissociating molecule generating the high-J CCl fragment. There is a 1^3A_1 state close in energy to the $\tilde{C}^1B_2$ and $\tilde{D}^1A_1$ states and strong state interaction is unavoidable. The 1^3A_1 state should be involved in the 248 nm photodissociation.

The next state which is electric-dipole allowed is 3^1A_1 state with VTE of 6.103 eV and calculated oscillator strength of about 0.00335. This state can be assigned as the state excited in the 193 nm photodissociation (photon energy of 6.42 eV) [30]. The 3^1A_1 state (the $4^1A'$ state in the C_s point group) is a predissociation electronic state and has an energy minimum at about 165° according to the calculated PES along the Cl–C–Cl bond angle. Applying

Table 2
VTE, Oscillator strength, electron configuration, and transition of electronic states of CCl_2.

State[a]	VTE	Oscillator strength	Main configuration	Excitation[b]
$1^1A'(1^1A_1)$	0		$(13–14a')^2(3–4a'')^2(15–16a')^2$	
$1^3A''(1^3B_1)$	1.245		$(15a')^2(16a')(5a'')$	$16a' \rightarrow 5a''$ (0.925)
$1^1A''(1^1B_1)$	2.605	0.00625	$(15a')^2(16a')(5a'')$	$16a' \rightarrow 5a''$ (0.890)
$2^3A''(1^3A_2)$	4.434		$(4a'')^2(15a')(16a')^2(5a'')$	$15a' \rightarrow 5a''$ (0.887)
$2^1A''(1^1A_2)$	4.487	1.82e−9	$(4a'')^2(15a')(16a')^2(5a'')$	$15a' \rightarrow 5a''$ (0.879)
$1^3A'(1^3B_2)$	4.88		$(3a'')^2(4a'')(15a'\text{-}16a')^2(5a'')$	$4a'' \rightarrow 5a''$ (0.903)
$2^1A'(1^1B_2)$	5.516	0.0748	$(3a'')^2(4a'')(15–16a')^2(5a'')$	$4a'' \rightarrow 5a''$ (0.807)
$2^3A'(1^3A_1)$	5.567		$(15a')^2(16a')(17a')$	$16a' \rightarrow 17a'$ (0.793)
$3^1A'(2^1A_1)$	5.606	0.00491	$(3–4a'')^2(15a')^2(5a'')^2$	$(16a')^2 \rightarrow (5a'')^2$ (0.834)
$4^1A'(3^1A_1)$	6.103	0.00335	$(15a')^2(16–17a')$	$16a' \rightarrow 17a'$ (0.599)
			$(14a')^2(3a'')(4a'')^2(15–16a')^2(5a'')$	$3a'' \rightarrow 5a''$ (0.225)
$3^3A'(2^3A_1)$	6.263		$(14a')^2(3a'')(4a'')^2(15–16a')^2(5a'')$	$3a'' \rightarrow 5a''$ (0.869)
$4^3A'(2^3B_2)$	6.460		$(15a')^2(16a')(18a')$	$16a' \rightarrow 18a'$ (0.789)
$3^3A''(2^3B_1)$	6.521		$(13a')(14a')^2(3–4a'')^2(15–16a')^2(5a'')$	$13a' \rightarrow 5a''$ (0.787)
$3^1A''(2^1B_1)$	6.769	0.00834	$(13a')(14a')^2(3–4a'')^2(15–16a')^2(5a'')$	$13a' \rightarrow 5a''$ (0.774)
$5^3A'(3^3B_2)$	6.993		$(4a'')^2(15a'\text{-}16a')(5a'')^2$	$15a',16a' \rightarrow (5a'')^2$ (0.613)
			$(4a'')^2(15a')(16a')^2(17a')$	$15a' \rightarrow 17a'$ (0.255)
$5^1A'(2^1B_2)$	7.234	0.00011	$(4a'')^2(15–16a')(5a'')^2$	$15a',16a' \rightarrow (5a'')^2$ (0.739)
$4^3A''(2^3A_2)$	7.427		$(13a')^2(14a')(3–4a'')^2(15–16a')^2(5a'')$	$13a' \rightarrow 5a''$ (0.676)
			$(3a'')^2(4a'')(15a')^2(16a')(5a'')^2$	$4a'', 16a' \rightarrow (5a'')^2$ (0.167)
$4^1A''(2^1A_2)$	7.485	1.11e−6	$(3a'')^2(4a'')(15a')^2(16a')(5a'')^2$	$4a'', 16a' \rightarrow (5a'')^2$ (0.470)
			$(13a')^2(14a')(3–4a'')^2(15–16a')^2(5a'')$	$14a' \rightarrow 5a''$ (0.422)
$5^3A''(3^3A_2)$	7.737		$(13a')^2(14a')(3–4a'')^2(15–16a')^2(5a'')$	$14a' \rightarrow 5a''$ (0.174)
			$(3a'')^2(4a'')(15a')^2(16a')(5a'')^2$	$4a'', 16a' \rightarrow (5a'')^2$ (0.449)
			$(3a'')^2(4a'')(15–16a')^2(17a')$	$4a'' \rightarrow 17a'$ (0.200)
$5^1A''(3^1A_2)$	8.205	3.25e−7	$(3a'')^2(4a'')(15a')^2(16a')(5a'')^2$	$4a'', 16a' \rightarrow (5a'')^2$ (0.186)
			$(13a')^2(14a')(3–4a'')^2(15–16a')^2(5a'')$	$14a' \rightarrow 5a''$ (0.289)
			$(3a'')^2(4a'')(15–16a')^2(17a')$	$4a'' \rightarrow 17a'$ (0.365)

[a] The symbol in parentheses refers to the representation of each state in the C_{2v} point group.
[b] The value in parentheses refers to the coefficient of the corresponding configuration.

the modified impulsive model [52] which can calculate the ratio of the rotational energy E_{rot} to the available energy E_{avl} using Eq. (1),

$$E_{rot}/E_{avl} = \frac{(m_{Cl})^2 \sin^2\theta}{(m_{Cl}+m_C)^2 - (m_{Cl})^2\cos^2\theta} \quad (1)$$

(where θ is the molecular bond angle), we predict that about 7.8% of the available energy would appear as CCl rotational energy. Our prediction is consistent with the experimental data (5–6%). Curve crossings along C–Cl coordinate between 3^1A_1 state and the repulsive electronic states including the singlet electronic state 2^1B_1 (the $3^1A''$ state in the C_s point group) and the triplet electronic states 2^3A_1 and 2^3B_1 (the $3^3A'$ and $3^3A''$ state in the C_s point group) as well as the coupling in avoided crossing between 3^1A_1 state and $\tilde{D}^1A_1$ state are observed from Fig. 2. The PESs of the 2^1B_1, 2^3A_1, 2^3B_1 and $\tilde{D}^1A_1$ states emanate from the ground $CCl(X^2\Pi) + Cl$ asymptote and CCl_2 may dissociate to the $CCl(X^2\Pi) + Cl$ along these repulsive PESs. Future work is necessary to be carried out to reveal the complicated dynamics of high excited states of CCl_2 radical.

4. Conclusions

In conclusion, the equilibrium geometries, transition energies for seven electronic states, $\tilde{X}^1A_1$, $\tilde{A}^1B_1$, $\tilde{a}^3B_1$, $\tilde{B}^1A_2$, $\tilde{b}^3A_2$, $\tilde{C}^1B_2$ and $\tilde{c}^3B_2$ of CCl_2 were calculated at the icMRCI+Q level with basis sets aug-cc-pV(X+d)Z, (X = T, Q, 5) and extrapolation to the CBS. Due to different electron transitions, the geometries of different states have large difference. Our ab initio structures have reproduced the experimental data and are in good agreement with the previous theoretical work. The energies also agree well with the experimental and theoretical data. For the first time, the PESs of high excited state of CCl_2 along the C–Cl bond distance and the Cl–C–Cl bond angle were examined at the icMRCI+Q/aug-cc-pV(5+d)Z level. The vertical transition energies, electronic configurations, and oscillator strengths of corresponding state were investigated at the same level.

Conflict of interest

There is no conflict of interest.

Acknowledgments

This work was supported by 2014 Postdoctoral Sustentation Fund of Qingdao, China and National Natural Science Foundation of China (11447148).

References

[1] H. Tomioka, Reactive Chemical Intermediates, Wiley and Sons, Hoboken, New Jersey, 2004 (Chapter 9).
[2] S.H. Kable, S.A. Reid, T.J. Sears, Int. Rev. Phys. Chem. 28 (2009) 435.
[3] H. Fan, I. Ionescu, C. Annesley, S.A. Reid, Chem. Phys. Lett. 378 (2003) 548.
[4] H. Fan, C. Mukarakate, M. Deselnicu, C. Tao, S.A. Reid, J. Chem. Phys. 123 (2005) 014314.
[5] M.K. Gilles, K.M. Ervin, J. Ho, W.C. Lheberger, J. Phys. Chem. A 96 (1992) 1130.
[6] T. Ibuki, A. Hiraya, K. Shobatake, Y. Matsumi, M. Kawasaki, J. Chem. Phys. 92 (1990) 4277.
[7] T.W. Schmidt, G.B. Bacskay, S.H. Kable, Chem. Phys. Lett. 292 (1998) 80.
[8] C. Tao, M. Deselnicu, H. Fan, C. Mukarakate, I. Ionescu, S.A. Reid, Phys. Chem. Chem. Phys. 8 (2006) 707.
[9] J.C. Poutsma, J.A. Paulino, R.R. Squires, J. Phys. Chem. A 101 (1997) 5327.
[10] K. Sendt, T.W. Schmidt, G.B. Bacskay, Int. J. Quantum Chem. 76 (2000) 297.
[11] C.S. Lin, Y.E. Chen, B.C. Chang, J. Chem. Phys. 121 (2004) 4164.
[12] B.-C. Chang, J. Guss, T.J. Sears, J. Mole. Spect. 219 (2003) 136.
[13] G.B. Bacskay, J. Phys. Chem. A 114 (2010) 8625.
[14] C. Wang, C. Chen, J. Dai, X. Ma, Chem. Phys. Lett. 288 (1998) 473.
[15] R.L. Schwartz, G.E. Davico, T.M. Ramond, W.C. Lineberger, J. Phys. Chem. A 103 (1999) 8213.
[16] F. Innocenti, M. Eypper, E.P. Lee, S. Stranges, D.K. Mok, F.T. Chau, G.C. King, J.M. Dyke, Chem. Eur. J. 14 (2008) 11452.
[17] F.T. Chau, D.K. Mok, E.P. Lee, J.M. Dyke, Chem. Phys. Chem. 6 (2005) 2037.
[18] F.-T. Chaua, J.M. Dykeb, E.P.-F. Leea, D.-C. Wang, J. Electron Spectrosc. Relat. Phenom. 97 (1998) 33.
[19] I. Rozum, N.J. Mason, J. Tennyson, J. Phys. B: At. Mol. Opt. Phys. 35 (2002) 1583.
[20] M. Mujitake, E. Hirota, J. Chem. Phys. 91 (1989) 3426.
[21] D.J. Clouthier, J. Karolczak, J. Chem. Phys. 94 (1991) 1.
[22] Z.-L. Cai, X.-G. Zhang, X.-Y. Wang, Chem. Phys. Lett. 210 (1993) 481.
[23] M. Fujitake, E. Hirota, J. Chem. Phys. 91 (1989) 3426.
[24] J.S. Guss, C.A. Richmond, K. Nauta, S.H. Kable, Phys. Chem. Chem. Phys. 7 (2005) 100.
[25] K. Sendt, G.B. Bacskay, J. Chem. Phys. 112 (2000) 2227.
[26] B.-S. Cheong, H.-G. Cho, J. Phys. Chem. A 101 (1997) 7901.
[27] M.L. McKee, J. Michl, J. Phys. Chem. A 106 (2002) 8495.
[28] G.P. Morley, P. Felder, J.R. Huber, Chem. Phys. Lett. 219 (1994) 195.
[29] C. Richmond, C. Tao, C. Mukarakate, H. Fan, K. Nauta, T.W. Schmidt, S.H. Kable, S.A. Reid, J. Phys. Chem. A 112 (2008) 11355.
[30] S.K. Shin, P.J. Dagdigian, J. Chem. Phys. 125 (2006) 133317.
[31] S.K. Shin, P.J. Dagdigian, Phys. Chem. Chem. Phys. 8 (2006) 3446.
[32] S.K. Shin, P.J. Dagdigian, J. Chem. Phys. 128 (2008) 154322.
[33] E.H. Al-Samra, C.M. Western, J. Mol. Spectrosc. 260 (2010) 135.
[34] J.M. Standard, R.J. Steidl, M.C. Beecher, R.W. Quandt, J. Phys. Chem. A 115 (2011) 1243.
[35] J.S. Guss, O. Votava, S.H. Kable, J. Chem. Phys. 115 (2001) 11118.
[36] R. Schlachta, G.M. Lask, V.E. Bondybey, J. Chem. Soc., Faraday Trans. 87 (1991) 2407.
[37] S.K. Shin, P.J. Dagdigian, J. Chem. Phys. 126 (2007) 134302.
[38] E. Sun, R. Li, Q. Sun, C. Wei, H. Xu, B. Yan, J. Phys. Chem. A 116 (2012) 10435.
[39] B.S. Truscott, N.L. Elliott, C.M. Western, J. Chem. Phys. 130 (2009) 234301.
[40] P.T. Knepp, C.K. Scalley, G.B. Bacskay, S.H. Kable, J. Chem. Phys. 109 (1998) 2220.
[41] J.M. Standard, R.W. Quandt, J. Phys. Chem. A 107 (2003) 6877.
[42] E. Sun, H. Lv, D. Shi, C. Wei, H. Xu, B. Yan, J. Phys. Chem. A 118 (2014) 2447.
[43] M. Schwartz, P. Marshall, J. Phys. Chem. A 103 (1999) 7900.
[44] S.K. Shin, P.J. Dagdigian, J. Chem. Phys. 128 (2008) 064309.
[45] G. Tarczay, T.A. Miller, G. Czako, A.G. Csaszar, Phys. Chem. Chem. Phys. 7 (2005) 2881.
[46] H.-J. Werner, P.J. Knowles, et al., MOLPRO, a package of ab initio programs, 2012.
[47] P.J. Knowles, H.-J. Werner, Chem. Phys. Lett. 145 (1988) 514.
[48] H.-J. Werner, P.J. Knowles, J. Chem. Phys. 89 (1988) 5803.
[49] S.R. Langhoff, E.R. Davidson, Int. J. Quantum Chem. 8 (1974) 61.
[50] J.T.H. Dunning, J. Chem. Phys. 90 (1989) 1007.
[51] J.T.H. Dunning, K.A. Peterson, A.K. Wilson, J. Chem. Phys. 114 (2001) 9244.
[52] H.B. Levene, J.J. Valentini, J. Chem. Phys. 87 (1987) 2594.